Glasslike Dynamics of Polar Domain Walls in Cryogenic $SrTiO_3$

David Pesquera, Michael A. Carpenter, and Ekhard K. H. Salje
Department of Earth Sciences, University of Cambridge, Downing Street, Cambridge CB2 3EQ, United Kingdom

(Received 27 August 2018; published 3 December 2018)

Polar and highly mobile domain walls in $SrTiO_3$ move under electric and elastic fields. Two vastly different timescales dominate their dynamical behavior. The previously observed fast changes lead to anomalies near 40 K where the elastic moduli soften and the polarity of the walls becomes strong. Keeping the sample under isothermal conditions leads to a new and unexpected phenomenon: The softening vanishes over timescales of days while the piezoelectricity of the sample remains unchanged. The hardening follows glass dynamics below an onset at $T^* \approx 40$ K. The timescale of the hardening is strongly temperature dependent and can be followed experimentally down to 34 K when the relaxation is not completed within two days. The relaxation time of a stretched exponential decay increases exponentially with the decreasing temperature. This relaxation process follows similar dynamics after zero-field cooling and after applying or removing an electric field. The sluggish behavior is attributed to collective interactions of domain patterns following overdamped glass dynamics rather than ballistic dynamics.

DOI: 10.1103/PhysRevLett.121.235701

The local structure of twin walls in $SrTiO_3$ is known only in an approximative toy model, while their true structural state is still unclear. One discovery has been that even the bulk structure is not tetragonal as had been assumed since 1968 [1]. Instead, small Sr displacements along [111] directions convoluted with counterrotations of the TiO_6 octahedra cause a local reduction in symmetry to triclinic, with point group symmetry 1. This locally triclinic structure was measured by ^{87}Sr NMR [2] and is relevant as it impacts noncentrosymmetric superconductivity in $SrTiO_3$, a subject of recently renewed interest [3]. It also coincides roughly with the onset of polarity inside the domain walls, which was predicted by Morozovska *et al.* [4] based on coupling between the gradient of the ferroelastic order parameter and the polar displacement and by considering biquadratic coupling between octahedral tilting and polarization [5,6]. This coupling increases the thickness of the domain walls, which, in turn, enhances their mobility, leading to elastic softening and acoustic dissipation, as evidenced in mechanical spectroscopy measurements [7]. Confirmation of emerging polarity in the walls was provided later by the detection of electrically generated mechanical resonances [8] and by local imaging of current flow [9], both enhanced below 40 K.

Domain walls display broken inversion symmetry inside the walls, even while the bulk ferroelastic domains are centrosymmetric [10–12]. They can hence be manipulated by an electric field [13]. Similar polar effects in twin walls have been observed in other perovskites, namely, $CaTiO_3$ [14] and $LaAlO_3$ [15,16]. They form the basis of emerging properties of internal interfaces as established in "domain boundary engineering" to generate novel functional materials (superconductors, memories, and transistors, to name but a few) [17]. Recently, Schiaffino and Stengel [18] identified two further mechanisms that contribute to wall polarity in $SrTiO_3$: a direct "rotopolar" coupling to the gradients of the antiferrodistortive octahedral tilts and a trilinear coupling that is mediated by the antiferroelectric displacement of the Ti atoms. Rotopolar coupling presents an analogy to the mechanism that generates a spontaneous polarization in cycloidal magnets. Vortex structures next to domain walls have been simulated by Zhao *et al.* [19] and were shown to depend sensitively on the presence of external electric fields. $SrTiO_3$ has therefore become a model system for exploring wall properties as a very promising candidate for emerging polar and superconducting functionalities.

Here we present experimental evidence from resonant ultrasound spectroscopy (RUS) [20] and resonant piezoelectric spectroscopy (RPS) [21] to show that elastic softening and increased damping associated with the polar ordering and enhanced mobility of domain walls below ~40 K in $SrTiO_3$ is not an equilibrium state. We find that this softening, observed either as appearing spontaneously when cooling or induced by applying an electric field, almost completely disappears after a slow dynamic process that drives the system towards the equilibrium state. The relaxation takes place on timescales which are much longer than previously identified for electric-field-induced domain reconfigurations [22]. It is shown to follow statistics characteristic of glassy systems, indicative of dynamic interactions within a dense network of domain walls and slowly evolving coupling of ferroelastic and ferroelectric order parameters.

We first confirmed the data for a single crystal $SrTiO_3$ sample in Ref. [8] for constant cooling rates. Experimental

details are given in the Supplemental Material [23]. RUS data display elastic softening and increased damping at the bulk structural transition temperature $T_c = 106$ K and at the temperature associated with incipient polarity in the domain walls $T^* \approx 40$ K, as shown in Fig. S2 of the Supplemental Material [23]. The new data show an additional anomaly at $T_f = 15.5$ K, which was not previously reported in elasticity measurements on $SrTiO_3$. It consists of a small increase in the resonance frequency and a peak in attenuation, which are characteristic features of a Debye loss process due to immobilization of defects coupled with shear strain such as is associated, for example, with pinning or freezing of domain walls [32]. The evaluation of the peak profile (Supplemental Material [23]) leads to an activation energy of 14 meV. RPS measurements confirmed the enhanced piezoelectric signals around T^*, following the same softening pattern as in RUS (Fig. S2 in the Supplemental Material [23]).

In order to test for kinetic effects associated with the structure which develops below $T^* \approx 40$ K, the evolution of RUS and RPS signals was followed at constant temperature in a series of separate experiments [33]. In each case, the sample was cooled from 70 K at a rate of ~0.3 K/ min and the cooling process halted at a chosen temperature. The start for isothermal data collection was taken to be the time at which the sample temperature became stable to better than 0.1 K for 1 min. No changes of resonance frequencies were found above 50 K under these isothermal conditions. At lower temperatures, systematic stiffening (increasing f^2) of the structure occurred as a function of time [Fig. 1(a)]. At long times, this stiffening substantially compensates for the softening observed near 40 K when changing temperature so that a fully relaxed sample would show a lesser degree of softening below T^*. The time evolution of data from RUS and RPS is virtually identical [data points in Fig. 1(b)] and can be described with integrated log-normal and stretched exponential functions. These functions are typical for glassy relaxations representing pinning or depinning events with a log-normal probability distribution function [34]. A stretched exponential typically occurs when very wide distributions of activation energies dominate the kinetic process [35]. Both functional forms coincide in $SrTiO_3$ and produce good fits to the data. As shown in Fig. 1(b), a stretched exponential of the form

$$f^2(t) = f_\infty^2 - (f_\infty^2 - f_0^2)\exp\left[-(t/\tau)^\beta\right] \qquad (1)$$

fits the time dependence of $f^2(t)$ at each temperature. This allows for initial f_0^2 and final values of f^2, f_∞^2 to be estimated [Fig. 1(c)]; τ is a relaxation time and β is a power factor.

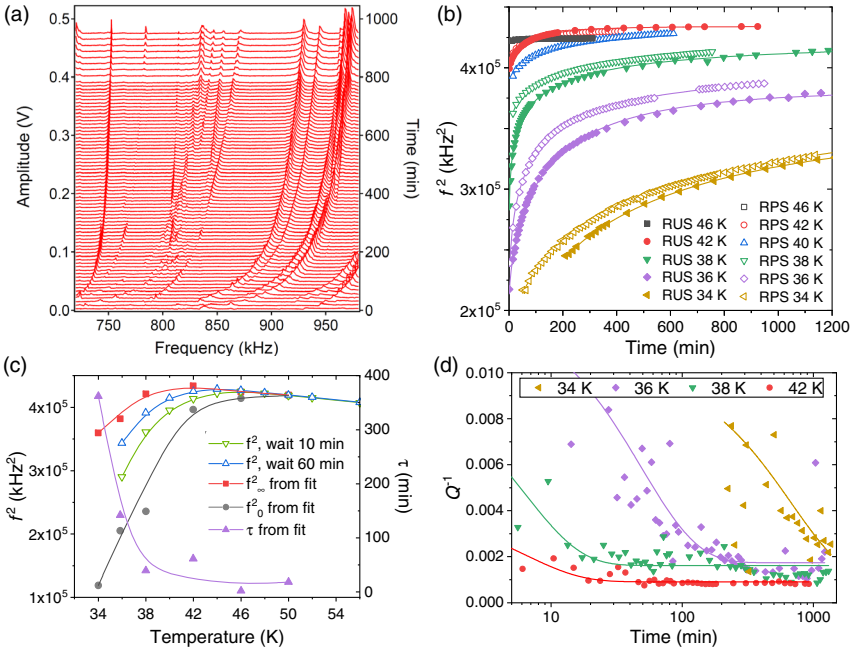

FIG. 1. (a) Time evolution of RPS spectra: Segments of the primary spectra have been offset up the y axis in proportion to the waiting time after thermal stabilization at the measurement temperature (36 K in this case). (b) f^2 variations for peak 2 as a function of time at different temperatures: filled symbols are RUS and open symbols are RPS. Lines are fits of Eq. (1). (c) Temperature dependence of the initial and equilibrium state values of f^2 (left axis) extracted from the fitting to the data in (b). Corresponding relaxation times are given on the right axis. Also shown (left axis) are the temperature dependences of f^2 for cooling sequences with delay times at each temperature before data collection of 10 min (green, downward triangles) and 60 min (blue, upward triangles). (d) Evolution of Q^{-1} with time at different temperatures from RUS. In (c) and (d), lines are guides to the eye.

The f_∞^2 values represent equilibrium and show a substantially weaker temperature dependence below 50 K, which means that the observed softening below 50 K is due to nonequilibrium states. This is consistent with the observation that the temperature T^*, at which softening begins, depends on the delay time allowed before collecting a spectrum during heating and cooling sequences. The data shown in Supplemental Material Fig. S2 [23] were collected with a delay time of 10 min after thermal stabilization at each temperature and are reproduced in Fig. 1(c) (downward-pointing triangles). T^* is lower for measurements taken with a delay time of 60 min at each temperature (upward-pointing triangles).

Below 38 K the relaxation becomes too sluggish to allow an approach to equilibrium during the approximately two days in which it was followed, so that the extracted f_∞^2 value is poorly determined. The average value of the power factor β obtained from the fittings was 0.48 ± 0.15, which is close to the factor found in simulations of jerk energy distributions in ferroelastic crystals at the crossover between elastic and plastic regimes [35]. The relaxation time τ extracted from the fitting to equation (1) appears to increase exponentially with decreasing temperature [Fig. 1(c)] and roughly displays Arrhenius dependence, as shown in Fig. S4 in the Supplemental Material [23], from which an estimation of the activation energy of the freezing process yields $E_a = 13$ meV, remarkably close to the activation energy extracted from the Debye loss peak at $T_f = 15.5$ K of the low-temperature RUS peak. This suggests similar freezing mechanisms occurring at T^* and T_f for different time spans.

Attenuation observed below T^* also changes during the relaxation, as indicated by decreasing resonance peak widths with increasing time at each temperature. Scatter in the data prevented reliable fitting, but the evolution of Q^{-1} can be represented as an exponential decrease with time [Fig. 1(d)]. The trends of increasing f^2 [Fig. 1(b)] and decreasing Q^{-1} [Fig. 1(d)] are clearly related and can be understood in terms of a progressive pinning process that counteracts the initial softening promoted by the enhanced mobility of the domain walls due to the changes in their internal structure below ~40 K. No decay in the RPS amplitude was identified with time, indicating that the piezoelectric effect persists after the relaxation process and, hence, that the polar ordering of the domain walls is stable. A relaxation mechanism due to an instability of the polar component, such as reported for $Na_{0.5}Bi_{0.5}TiO_3$ [36], can, therefore, be discarded here.

The effect of an electrical perturbation on the relaxation process was tested by applying a fixed dc voltage across the $SrTiO_3$ crystal while collecting RUS spectra (see the experimental details in the Supplemental Material [23]). The time evolution of the RUS signal at 36 K after cooling in zero electric field from 70 K [red spectra in Fig. 2(a)] was altered significantly when an electric field of 1 kV/cm was applied 314 min after thermal stabilization, interrupting the smooth relaxation and inducing a sudden softening evidenced in all resonance peaks detected. After the abrupt frequency shift induced by the electric field, the relaxation process restarted [purple spectra in Fig. 2(a)], following a similar time dependence as the initial relaxation at zero field. Removing the electric field after another 314 min equally caused a sudden softening and resetting of the relaxation [green spectra in Fig. 2(a)].

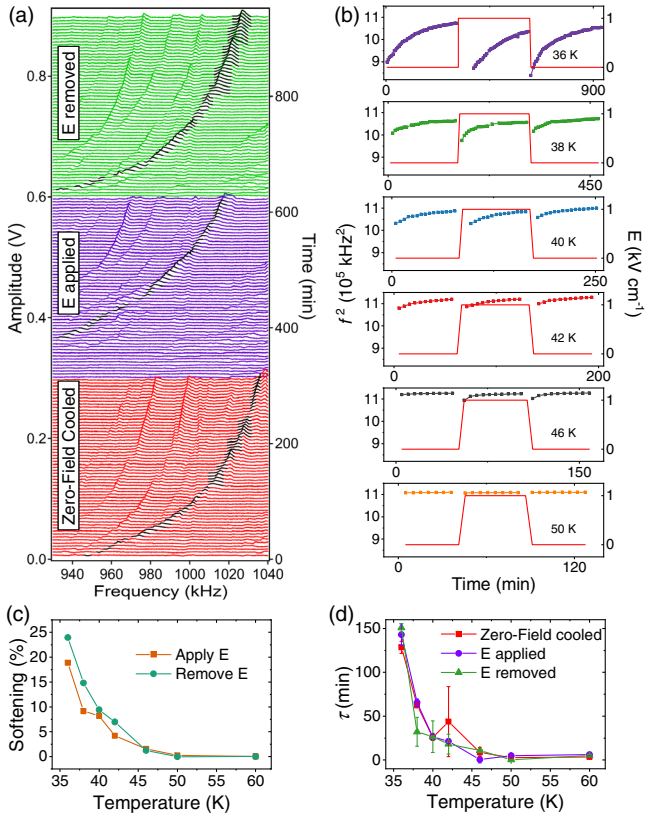

FIG. 2. Influence of dc field on isothermal evolution at different temperatures. (a) Time evolution of RUS spectra at 36 K after cooling from 70 K. The elastic relaxation observed initially (red spectra) is reset when an electric field is applied (purple) and when this field is removed (green). Segments of spectra have been offset up the y axis in proportion to the waiting time after thermal stabilization at 36 K. Black lines are fits to one of the resonance peaks. (b) Time evolution of f^2 for the resonance shown in (a) at different temperatures (dots joined by lines, left axis) and corresponding time sequence of applied electric field across the crystal (red lines, right axis). (c) Softening caused by applying or removing the electric field as a function of the temperature. (d) Relaxation time extracted from fits to data in (b) as a function of the temperature.

The temperature dependence of the field-induced effect on the relaxation was explored between 36 and 60 K. A significant field-induced softening was observed only below 50 K, becoming more relevant at lower temperatures. All relaxations (with and without applied electric field) could be fitted to Eq. (1), and the softening caused by the

electric field change was estimated as the difference between the last f^2 value observed prior to application or removal of the field and the initial f^2 value of the next relaxation process (either corresponding to f_0^2 or to the observed value in the spectra). The magnitude of the softening increases exponentially with decreasing temperature [Fig. 2(c)] in a similar fashion to the relaxation time τ extracted from the fits to all three relaxations per temperature [Fig. 2(d)].

The applied dc electric field used in our experiments was deemed too small to induce a ferroelectric phase [37] or to produce a significant variation in the number of vortex structures that might nucleate between twin boundaries [19]. More overtly, both effects would be expected to be revealed by different elastic responses between zero-field cooling and field cooling conditions, which were not identified in our experiments, as evidenced in Fig. S5 of the Supplemental Material [23]. Most likely, the effect of applying and removing the small electric field at low temperatures is to cause a change in the domain patterns, as observed by Casals *et al.* [38] and Honig *et al.* [39]. This, in turn, will reset the relaxation process in which the domain walls experience viscous drag as they evolve towards their new equilibrium configuration. Even though the new microstructure may be different after applying or removing the electric field [38,39], it has been found here that the relaxation process towards the equilibrium state follows closely similar dynamics after zero-field cooling and after applying or removing an electric field.

In summary, the spontaneous formation of polar structures at the twin boundaries of $SrTiO_3$ shows a dynamic coupling with strain. An elastic softening associated with the internal changes in the structure of the domain walls increasing their mobility is gradually outweighed by a sluggish relaxational process involving elastic stiffening and reduction of acoustic loss (i.e., slow freezing). The relaxation time associated with slowing down of the microstructure changes is abnormally large at temperatures immediately below the emergence of polarity in the walls and is identified as a progressive evolution of the elastic constants with time. At lower temperatures, the mobility of the twin walls is reduced within the time constant of the elasticity measurements and, therefore, identified as a peak in the temperature dependence of the loss. Similar activation energies estimated for both "slow" and "fast" freezing processes point to a single pinning mechanism with a relaxation time strongly dependent on the temperature.

This relaxation is important as it is indicative of enhanced interactions within the multiferroic (ferroelastic+ferroelectric) microstructure of $SrTiO_3$ at low temperatures. A possible scenario to explain these dynamics involves the nucleation and propagation of polar vortex structures, as observed in simulations [40,41], which may cause jamming or pinning with charged defects. At fixed temperatures, small electric fields restore the mobility of the domain walls, but the system is then driven to the equilibrium state following the same relaxation dynamics as when changing the temperature, which may be determined exclusively by the number of polar vortices nucleated in the structure. Direct observation of such polar structures is challenging [42], and their stability strongly depends on domain configurations [40,43]; however, we hope that our evidence for ultraslow elastic relaxations may inspire new experiments that explore the stress-polarization coupling due to the nucleation of local polar structures in a nonpolar material [9]. These results may also inspire studies of magnetoelastic coupling in jammed magnetic systems [44,45] or strain coupling in slowly relaxing structures [46,47], which show similar dynamics to the $SrTiO_3$ domain glass state.

This work was funded by EPSRC Grant No. EP/P024904/1, which is gratefully acknowledged. RUS facilities in Cambridge were established through grants from the Natural Environment Research Council (Grants No. NE/B505738/1 and No. NE/F017081/1) and the Engineering and Physical Sciences Research Council (Grant No. EP/I036079/1) to M. A. C.

[1] P. A. Fleury, J. F. Scott, and J. M. Worlock, Phys. Rev. Lett. **21**, 16 (1968).
[2] R. Blinc, B. Zalar, V. V. Laguta, and M. Itoh, Phys. Rev. Lett. **94**, 147601 (2005).
[3] H. Q. Yuan, D. F. Agterberg, N. Hayashi, P. Badica, D. Vandervelde, K. Togano, M. Sigrist, and M. B. Salamon, Phys. Rev. Lett. **97**, 017006 (2006).
[4] A. N. Morozovska, E. A. Eliseev, M. D. Glinchuk, L.-Q. Chen, and V. Gopalan, Phys. Rev. B **85**, 094107 (2012).
[5] B. Houchmandzadeh, J. Lajzerowicz, and E. Salje, J. Phys. Condens. Matter **3**, 5163 (1991).
[6] S. Conti, S. Müller, A. Poliakovsky, and E. K. H. Salje, J. Phys. Condens. Matter **23**, 142203 (2011).
[7] J. F. Scott, E. K. H. Salje, and M. A. Carpenter, Phys. Rev. Lett. **109**, 187601 (2012).
[8] E. K. H. Salje, O. Aktas, M. A. Carpenter, V. V. Laguta, and J. F. Scott, Phys. Rev. Lett. **111**, 247603 (2013).
[9] Y. Frenkel, N. Haham, Y. Shperber, C. Bell, Y. Xie, Z. Chen, Y. Hikita, H. Y. Hwang, E. K. H. Salje, and B. Kalisky, Nat. Mater. **16**, 1203 (2017).
[10] P. Barone, D. Di Sante, and S. Picozzi, Phys. Rev. B **89**, 144104 (2014).
[11] S. Baroni, S. De Gironcoli, A. Dal Corso, and P. Giannozzi, Rev. Mod. Phys. **73**, 515 (2001).
[12] N. A. Benedek and C. J. Fennie, Phys. Rev. Lett. **106**, 107204 (2011).
[13] J. Fontcuberta, V. Skumryev, V. Laukhin, X. Granados, and E. K. H. Salje, Sci. Rep. **5**, 13784 (2015).
[14] S. Van Aert, S. Turner, R. Delville, D. Schryvers, G. Van Tendeloo, and E. K. H. Salje, Adv. Mater. **24**, 523 (2012).
[15] E. K. H. Salje, M. Alexe, S. Kustov, M. C. Weber, J. Schiemer, G. F. Nataf, and J. Kreisel, Sci. Rep. **6**, 27193 (2016).

[16] H. Yokota, S. Matsumoto, E. K. H. Salje, and Y. Uesu, Phys. Rev. B **98**, 104105 (2018).
[17] G. Catalan, J. Seidel, R. Ramesh, and J. F. Scott, Rev. Mod. Phys. **84**, 119 (2012).
[18] A. Schiaffino and M. Stengel, Phys. Rev. Lett. **119**, 137601 (2017).
[19] Z. Zhao, X. Ding, and E. K. H. Salje, Appl. Phys. Lett. **105**, 112906 (2014).
[20] M. A. Carpenter, J. Phys. Condens. Matter **27**, 263201 (2015).
[21] E. K. H. Salje, M. A. Carpenter, G. F. Nataf, G. Picht, K. Webber, J. Weerasinghe, S. Lisenkov, and L. Bellaiche, Phys. Rev. B **87**, 014106 (2013).
[22] J. Sidoruk, J. Leist, H. Gibhardt, O. Sobolev, B. Ouladdiaf, R. Mole, and G. Eckold, Ferroelectrics **505**, 200 (2016).
[23] See Supplemental Material at http://link.aps.org/supplemental/10.1103/PhysRevLett.121.235701 for experimental details on RUS and RPS measurements, temperature evolution of RUS and RPS signals, Arrhenius behavior of relaxation times, and temperature dependence of RUS under zero-field and field cooling conditions, which includes Refs. [24–31].
[24] R. E. A. McKnight, M. A. Carpenter, T. W. Darling, A. Buckley, and P. A. Taylor, Am. Mineral. **92**, 1665 (2007).
[25] D. M. Evans, J. A. Schiemer, M. Schmidt, H. Wilhelm, and M. A. Carpenter, Phys. Rev. B **95**, 094426 (2017).
[26] O. Aktas, M. A. Carpenter, and E. K. H. Salje, Appl. Phys. Lett. **103**, 142902 (2013).
[27] O. Aktas, S. Crossley, M. A. Carpenter, and E. K. H. Salje, Phys. Rev. B **90**, 165309 (2014).
[28] M. Weller, G. Y. Li, J. X. Zhang, T. S. Kê, and J. Diehl, Acta Metall. **29**, 1047 (1981).
[29] R. Viana, P. Lunkenheimer, J. Hemberger, R. Böhmer, and A. Loidl, Phys. Rev. B **50**, 601 (1994).
[30] M. Maglione, Ferroelectrics **254**, 151 (2001).
[31] P. Zubko, G. Catalan, A. Buckley, P. R. L. Welche, and J. F. Scott, Phys. Rev. Lett. **99**, 167601 (2007); **100**, 199906(E) (2008).
[32] R. J. Harrison, S. A. T. Redfern, A. Buckley, and E. K. H. Salje, J. Appl. Phys. **95**, 1706 (2004).
[33] E. K. H. Salje, H. Liu, L. Jin, D. Jiang, Y. Xiao, and X. Jiang, Appl. Phys. Lett. **112**, 054101 (2018).
[34] E. Faran, E. K. H. Salje, and D. Shilo, Appl. Phys. Lett. **107**, 071902 (2015).
[35] X. Ding, T. Lookman, Z. Zhao, A. Saxena, J. Sun, and E. K. H. Salje, Phys. Rev. B **87**, 094109 (2013).
[36] O. Aktas, J. R. Duclère, S. Quignon, G. Trolliard, and E. K. H. Salje, Appl. Phys. Lett. **113**, 032901 (2018).
[37] J. Sidoruk, J. Leist, H. Gibhardt, M. Meven, K. Hradil, and G. Eckold, J. Phys. Condens. Matter **22**, 235903 (2010).
[38] B. Casals, A. Schiaffino, A. Casiraghi, S. J. Hämäläinen, D. López González, S. van Dijken, M. Stengel, and G. Herranz, Phys. Rev. Lett. **120**, 217601 (2018).
[39] M. Honig, J. A. Sulpizio, J. Drori, A. Joshua, E. Zeldov, and S. Ilani, Nat. Mater. **12**, 1112 (2013).
[40] E. K. H. Salje, S. Li, Z. Zhao, P. Gumbsch, and X. Ding, Appl. Phys. Lett. **106**, 212907 (2015).
[41] E. K. H. Salje, S. Li, M. Stengel, P. Gumbsch, and X. Ding, Phys. Rev. B **94**, 024114 (2016).
[42] A. K. Yadav, C. T. Nelson, S. L. Hsu, Z. Hong, J. D. Clarkson, C. M. Schlepuëtz, A. R. Damodaran, P. Shafer, E. Arenholz, L. R. Dedon, D. Chen, A. Vishwanath, A. M. Minor, L. Q. Chen, J. F. Scott, L. W. Martin, and R. Ramesh, Nature (London) **530**, 198 (2016).
[43] Z. Hong, A. R. Damodaran, F. Xue, S. L. Hsu, J. Britson, A. K. Yadav, C. T. Nelson, J. J. Wang, J. F. Scott, L. W. Martin, R. Ramesh, and L. Q. Chen, Nano Lett. **17**, 2246 (2017).
[44] S.-W. Chen, H. Guo, K. A. Seu, K. Dumesnil, S. Roy, and S. K. Sinha, Phys. Rev. Lett. **110**, 217201 (2013).
[45] S. Konings, C. Schüßler-Langeheine, H. Ott, E. Weschke, E. Schierle, H. Zabel, and J. B. Goedkoop, Phys. Rev. Lett. **106**, 077402 (2011).
[46] E. K. H. Salje, D. J. Safarik, J. C. Lashley, L. A. Groat, and U. Bismayer, Am. Mineral. **96**, 1254 (2011).
[47] B. Ruta, E. Pineda, and Z. Evenson, J. Phys. Condens. Matter **29**, 503002 (2017).